

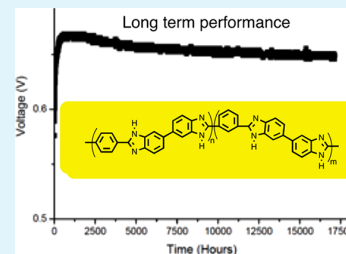
# Durable High Polymer Content *m/p*-Polybenzimidazole Membranes for Extended Lifetime Electrochemical Devices

Andrew T. Pingitore,<sup>1b</sup> Fei Huang, Guoqing Qian, and Brian C. Benicewicz\*<sup>1b</sup>

Department of Chemistry and Biochemistry, University of South Carolina, Columbia, South Carolina 29208, United States

**ABSTRACT:** A series of high polymer content phosphoric acid-doped *m/p*-polybenzimidazole (PBI) copolymer membranes were prepared via the poly(phosphoric acid) (PPA) process. These copolymer membranes showed much higher solubility in solution (7–10 wt %) compared to the homopolymer *para*-PBI (typically <3.5 wt %), which translated to higher polymer solids content in the PPA-processed doped membranes. Concurrent with these changes, the compressive creep compliance ( $J$ ) decreased from approximately  $1 \times 10^{-5}$  to  $<2 \times 10^{-6}$  Pa<sup>-1</sup>. These membranes exhibited high proton conductivities, >150 mS/cm at typical operating temperatures of 160–200 °C, and showed exceptional low voltage decay,  $\sim 0.67$   $\mu$ V/h when tested at 160 °C for more than 2 years.

**KEYWORDS:** polybenzimidazole, fuel cells, hydrogen purification, creep, PEMs, electrochemical devices



## INTRODUCTION

Phosphoric acid (PA)-doped polybenzimidazole (PBI) membranes have long been studied as high-temperature polymer electrolyte membranes (HT-PEMs), and considerable progress has been made in the past 10 years. Throughout this time many members of the PBI family were extensively investigated for use in high-temperature polymer electrolyte membrane fuel cells (HT-PEMFCs), which include *meta*-PBI,<sup>1</sup> *para*-PBI,<sup>2</sup> AB-PBIs,<sup>3,4</sup> partially fluorinated PBIs,<sup>5,6</sup> hydroxylated PBIs,<sup>7</sup> sulfonated PBIs,<sup>8</sup> pyridine PBIs,<sup>9–11</sup> and their copolymers. Compared to low-temperature polymer electrolyte membranes (LT-PEMs) based on perfluorosulfonic acid (PFSA) ionomers, such as Dupont's Nafion, PA-doped PBI membranes have high proton conductivity at high operational temperatures (up to 200 °C), low reactant permeability, high fuel impurity tolerance, excellent oxidative and thermal stability, and nearly zero electroosmotic drag coefficient<sup>12–17</sup> that are useful in multiple device applications. In this operational temperature range (120–200 °C) heat and water management is greatly simplified. Additionally, the reaction kinetics of the catalysts on the electrode increase with increasing temperature, which opens the possibility of using cheaper catalyst materials to replace the expensive platinum (Pt) electrode catalyst typically used in fuel cells.<sup>18</sup> Moreover, because of the high-temperature stability and strong acid resistance of the PBI family of polymers, they have been found to be good candidates for a variety of electrochemical devices other than fuel cells, for example, electrochemical hydrogen pumps and electrolyzers for the hybrid sulfur cycle.<sup>19–21</sup>

Traditionally, PA-doped PBI membranes are prepared from the *meta*-PBI polymer produced from a two-step melt–solid polymerization. The produced polymer powders are dissolved in a polar aprotic solvent, such as *N,N'*-dimethylacetamide (DMAc) at high temperatures. The solution is filtered to remove undissolved parts. The solution is then cast and the

solvent evaporated to obtain a dry membrane. Finally, the dry membranes are soaked in phosphoric acid to prepare the doped film. This time-consuming, costly, environmentally unfriendly, multistep process is termed the “conventional imbibing process”.<sup>22</sup> To mitigate the issues with this technique, Xiao et al. developed the novel “PPA process” to prepare phosphoric acid-doped PBI membranes.<sup>2</sup> This process uses poly(phosphoric acid) (PPA) for the polymerization of tetramines and diacids and optionally AB monomers. PPA is quite useful in these polymerizations as it is an excellent solvent for many PBIs, removes the water condensation product efficiently by reaction with the phosphate anhydride structure, and activates the acid functionality via formation of mixed phosphate anhydrides. Polymer molecular weights, as measured by inherent viscosity (IV), are typically high with IV values of 2–6 dL g<sup>-1</sup> often reported for many PBI structures. The high molecular weight polymer solution is cast immediately after polymerization while still at temperatures between 180 and 200 °C on suitable substrates to form thin (ca. 250  $\mu$ m) films. Exposure of the cast solution to atmospheric moisture or controlled humidity conditions allows moisture to be absorbed into the solution as both PBI and PPA are hygroscopic. The absorbed moisture hydrolyzes the PPA, a good solvent for PBI, to phosphoric acid (PA), a poor solvent for PBI, and induces a solution to gel transition, thus creating the gel film that is coincidentally and conveniently imbibed with the dopant PA. This process also results in PA doping levels that are higher (15–30 mol PA per mol polymer repeat unit) than those reported for conventionally imbibed membranes (<10 mol PA per mol polymer repeat unit). Thus, the PPA process is a simpler, less costly, and time-

**Received:** October 22, 2018

**Accepted:** February 7, 2019

**Published:** February 7, 2019

effective alternative process over the conventional imbibing method that also produces membranes with high proton conductivities due to the high phosphoric acid doping levels. Poly(2,2'-(1,4-phenylene)5,5'-bibenzimidazole) (*para*-PBI) membranes prepared by the PPA process have high proton conductivities ( $>0.25$  S/cm at  $160$  °C), which is attributed to their high phosphoric acid doping level ( $>20$  PA/PBI r.u.). Excellent fuel cell performances have also been demonstrated with these PA-doped *para*-PBI membranes—greater than  $0.65$  V at  $0.2$  A/cm<sup>2</sup> for hydrogen and air at  $160$  °C and lifetimes of at least 2 years under steady-state conditions.<sup>2,23</sup>

When considering PA-doped PBI membranes prepared via the conventional imbibing process, a trade-off between two key properties of the membrane is realized, i.e., proton conductivity and mechanical properties. For example, to obtain a high proton conducting membrane PA doping levels must be high, however, this leads to lower mechanical properties of the membrane. The “practical” phosphoric acid doping level of a conventionally imbibed membrane is  $\sim 6$ – $10$  mol of PA/PBI r.u., and the resulting membrane (at  $\sim 6$  PA/PBI r.u.) exhibited a  $11$  MPa Young’s modulus; however, the proton conductivity was only  $0.04$ – $0.06$  S/cm. With doping levels  $>6$  PA/PBI r.u., the membranes become very soft, and mechanical properties of the resulting membranes quickly dropped to levels too low to fabricate a membrane electrode assembly.<sup>22</sup>

More recently, Chen et al. conducted a thorough study characterizing the creep compliance of a multitude of PA-doped PBI membrane chemistries. The creep compliance of high-temperature PEMs is a relatively new aspect of characterizing films for long-term durability, as creep deformation was identified as the likely primary failure mode of PBI membranes prepared through the PPA process. Their work showed a strong correlation between the membranes final polymer content and its resistance to creep. For example, *para*-PBI membranes prepared via the PPA route have high PA doping levels ( $>20$  PA/PBI r.u.) and a polymer content of just  $4$ – $5$  wt %. The membrane mechanical properties were evaluated and showed a Young’s modulus of  $\sim 2$  MPa and creep compliance ( $J_s^0$ ) values of  $\sim 9.0 \times 10^6$  Pa<sup>-1</sup> from dynamic mechanical analysis. Furthermore, a direct correlation was found for *para*-PBI membranes where an increase in final polymer solids decreased creep deformation. A similar trend was also found for the *meta*-PBI family of polymer membranes; however, the more flexible chain linkage reduced the overall efficacy of polymer solids to lower creep compliance.<sup>24</sup>

Herein, we investigate a novel series of *meta/para*-PBI random copolymer membranes synthesized via the PPA process. Introducing the more soluble *meta*-PBI repeat unit into the less soluble *para*-PBI, in PPA, resulted in more concentrated copolymer/PPA solutions having processable viscosities and producing membranes with much higher polymer content. Membrane properties, i.e., proton conductivity, mechanical properties, and creep resistance, of these PA-doped *meta/para*-PBI copolymer gel membranes were explored and compared to *meta*-PBI membranes prepared via the conventional imbibing process and *para*-PBI membranes prepared by the PPA process. This work proposes that the mechanical properties, i.e., creep, of the membrane are more associated with the voltage degradation and overall lifetime of PBI gel membranes and that under these time constraints the PA loss rate is not the main cause for the decrease in performance.<sup>25</sup> The new membranes were also tested in

different electrochemical devices such as high-temperature PEM fuel cells and electrochemical hydrogen pumps.

## EXPERIMENTAL SECTION

**Materials.** 3,3',4,4'-Tetraaminobiphenyl (TAB, polymer grade,  $\sim 97.5\%$ ) was donated by BASF Fuel Cell, Inc. and used as received. Isophthalic acid (IPA,  $>99\%$  purity) and terephthalic acid (TPA,  $>99\%$  purity) were purchased from Amoco and used as received. Poly(phosphoric acid) (115%) was supplied from FMC Corporation and used as received. Reformate test gas ( $30\%$  H<sub>2</sub>,  $3\%$  CO,  $67\%$  N<sub>2</sub>, mol %) was mixed by AirGas and used as received.

**Polymer Synthesis and Membrane Fabrication.** A typical polymerization consisted of  $64.28$  g of tetraaminobiphenyl (TAB,  $300$  mmol),  $43.62$  g of isophthalic acid (IPA,  $262.5$  mmol), and  $6.23$  g of terephthalic acid (TPA,  $37.5$  mmol) added to  $1050$  g of poly-(phosphoric acid), mixed with an overhead stirrer and purged with dry nitrogen. The contents were heated in a high-temperature silicone oil bath, and the temperature was controlled by a programmable temperature controller with ramp and soak features. In a typical polymerization, the final reaction temperature was  $\sim 195$  °C and held for  $12$  h. Once the reaction was completed, determined by visual inspection of viscosity, the polymer solution was cast onto clear glass plates using a doctor blade with a controlled gate thickness of  $15$  mils. The cast solution was hydrolyzed into membranes in a humidity chamber regulated to  $55\%$  RH at  $25$  °C, where a sol–gel transition occurs trapping the polymer in a Flory Type III gel.<sup>2</sup> Typical final membrane thicknesses were in the range  $250$ – $280$   $\mu\text{m}$ .

**Inherent Viscosity (IV) Measurements.** Because of the low solubility of PBI polymers, IV measurements were taken to determine relative molecular weights. IVs were taken in a Cannon Ubbelohde viscometer in a temperature-controlled water bath ( $30$  °C). The polymers or copolymers were dissolved in concentrated sulfuric acid at a concentration of  $0.2$  g/L. Samples were passed through a  $0.25$   $\mu\text{m}$  PTFE syringe filter before injecting into the viscometer.

**Membrane Composition.** The composition of phosphoric acid-doped PBI membranes was determined by measuring the relative amounts of polymer solids, water, and acid in the membranes. The phosphoric acid (PA) content of a membrane was determined by titrating a membrane sample with standardized sodium hydroxide solution ( $0.10$  M) using a Metrohm 716 DMS Titrino autotitrator. Once titrated, the sample was thoroughly washed with DI water and dried at reduced pressures at  $120$  °C overnight. The dried sample was then weighed to determine the polymer solids content of the membrane.

The polymer weight percentage and phosphoric acid weight percentage can be determined via eqs 1 and 2:

$$\text{polymer wt \%} = \frac{W_{\text{dry}}}{W_{\text{sample}}} \times 100 \quad (1)$$

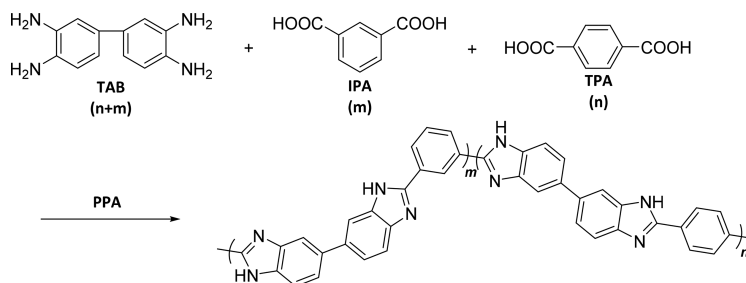
$$\text{acid wt \%} = \frac{M_{\text{acid}} V_{\text{NaOH}} c_{\text{NaOH}}}{W_{\text{sample}}} \quad (2)$$

where  $W_{\text{sample}}$  is the weight of the sample before titration,  $W_{\text{dry}}$  is the weight of final dried sample after titration,  $M_{\text{acid}}$  is the molecular weight of phosphoric acid, and  $V_{\text{NaOH}}$  and  $c_{\text{NaOH}}$  are the volume and concentration of the sodium hydroxide solution required to neutralize the phosphoric acid to the first equivalence point.

The number of moles of phosphoric acid per mole of PBI repeat unit (or the PA doping levels,  $X$ ) is calculated from the equation

$$X = \frac{V_{\text{NaOH}} c_{\text{NaOH}}}{W_{\text{dry}} / M_{\text{polymer}}} \quad (3)$$

where  $V_{\text{NaOH}}$  and  $c_{\text{NaOH}}$  are the volume and concentration of the sodium hydroxide solution required to neutralize the phosphoric acid to the first equivalence point,  $W_{\text{dry}}$  is the final weight of the dried sample after titration, and  $M_{\text{polymer}}$  is the molecular weight of the polymer repeat unit.

Scheme 1. Synthesis of *meta/para*-PBI in PPA<sup>a</sup>

<sup>a</sup>Detailed polymerization conditions are provided in Table 1.

**Tensile Properties.** The tensile properties of the membranes were tested at room temperature using an Instron Model 5543A system with a 10 N load cell and crosshead speed of 5 mm/min. Dog-bone-shaped specimens were cut according to ASTM standard D683 (Type V specimens) and preloaded to 0.1 N prior to testing.

**Compression Creep and Creep Recovery Experiment.** The compression creep and creep recovery method was used to study the time-dependent creep behavior of the prepared membranes in a TA RSA III dynamic mechanical analyzer using its built-in functionality for creep testing. A typical experiment consisted of a 20 h creep phase followed by a 3 h recovery phase. During the creep phase, a constant compressive force equivalent to a stress level of 0.1 MPa was applied, and this force was removed at the start of the recovery phase. All experiments were performed at  $180 \pm 0.5$  °C in a temperature-controlled oven with dry air circulation. The creep test was repeated 2–4 times for each gel membrane.

**Proton Conductivity.** Proton conductivities of the membrane were measured by a four-probe electrochemical impedance spectroscopy method using a Zahner IM6e electrochemical workstation over the frequency range from 1 Hz to 100 kHz with an amplitude of 5 mV. A two-component model with an ohmic resistance in parallel with a capacitor was employed to fit the experimental data. The conductivities of the membrane at different temperatures were calculated from the membrane resistance obtained from the model simulation with the following equation:

$$\sigma = \frac{d}{lwR_m} \quad (4)$$

where  $d$  is the distance between the two inner probes,  $l$  is the thickness of the membrane,  $w$  is the width of the membrane, and  $R_m$  is the ohmic resistance determined by the model fitting. Membrane samples underwent two heating ramps to 180 °C. Conductivity data reported were recorded on the second heat ramp after water was removed from the membrane during the first heating cycle.

**Membrane Electrode Assembly (MEA) Preparation and Fuel Cell Testing.** The gas diffusion electrodes (GDE, acquired from BASF Fuel Cell, Inc.) with a platinum loading of 1.0 mg/cm<sup>2</sup> were used for this study. Where applicable, the GDE was treated with a fluorinated PBI solution, where dry 6F-PBI powders were dissolved in DMAc (0.5 wt %) and sprayed onto BASF standard electrodes with a Badger air brush (model 100). The sprayed electrodes were dried under reduced pressures overnight (120 °C). The 6F-PBI loading on the electrodes used was 0.1 mg/cm<sup>2</sup>.<sup>26</sup> The MEA was fabricated by hot pressing a piece of membrane between two Kapton-framed electrodes. MEAs were then assembled into single cell fuel cell test equipment. The gas flow plates used were constructed from graphite with triple serpentine gas channels. Stainless steel end plates with attached heaters were used to clamp the graphite flow plates. A commercial fuel cell testing station (Fuel Cell Technology, Inc.) was used for cell testing. The instrument was controlled by home-programmed LabView software (National Instruments, Austin, TX). Fuel cell testing was conducted on 50 cm<sup>2</sup> cells, and electrochemical hydrogen pumping tests were conducted on 10 cm<sup>2</sup> cells.

**Phosphoric Acid Loss.** Condensed water from fuel cell operation was collected from both the anode and cathode at predetermined time intervals. A solution of ammonium molybdate (20 g) in water (500 mL), along with a solution of 0.1 M ascorbic acid, as well as a solution of potassium antimonyl tartrate (1.3715 g) in 400 mL of water were prepared. Once fully dissolved the solutions were slowly mixed together in the quantities 15, 30, and 5 mL, respectively, along with 50 mL of 5 N sulfuric acid. Water/phosphoric acid samples collected from the fuel cell were added to the mixed reagent solution. The absorbance at 880 nm was measured using a Shimadzu UV-2450 spectrophotometer where the absorbance correlates to the concentration of phosphoric acid.<sup>27</sup>

**Hydrogen Pump Operation.** MEA fabrication for electrochemical hydrogen pump tests was similar to that for fuel cells except they were constructed with symmetrical electrodes, 1 mg/cm<sup>2</sup> Pt on both the anode and cathode (BASF Fuel Cell, Inc.). The MEAs were assembled into the same cell hardware used for fuel cell performance testing. Polarization curves were recorded at 160, 180, and 200 °C with 1.25 stoichiometric flow of H<sub>2</sub> supplied to the anode and without a sweep gas applied to the cathode. MEAs were also subjected to a reformat test gas (30% H<sub>2</sub>, 3% CO, and 67% N<sub>2</sub>, mol %), incorporating large amounts of catalyst poisons that require higher operating temperatures.

## RESULTS AND DISCUSSION

**Polymer Synthesis and Membrane Fabrication.** The *meta/para*-PBI copolymers and membranes were prepared via the PPA process, as shown in Scheme 1.

*para*-PBI membranes prepared by the PPA process typically have only 4–5 wt % polymer content. Our group has previously shown that low polymer content leads to limiting creep and creep compliance properties of polymer gel membranes.<sup>24</sup> Two different techniques were attempted to increase final membrane solids: directly increasing monomer charge in the polymerization and by adding preformed *para*-PBI polymer powder to the polymerization during its later stages. However, these techniques limited processability of the PBI/PPA solution due to the low solubility of *para*-PBI in PPA and to the high viscosities of the final polymer solution. The upper limit of processability for hand casting *para*-PBI/PPA solutions was 2.8 wt % *para*-PBI content (3.5 wt % of monomer charge). By introduction of a more soluble *meta*-PBI repeat unit into the polymer backbone, higher monomer charges up to 10 wt % (or 8 wt % of polymer in the PBI/PPA casting solution) could be polymerized without any evidence of early polymer precipitation. These PBI/PPA solutions retained suitable viscosities to process into films, thus producing high polymer content phosphoric acid-doped PBI membranes. The monomer ratio was also used to adjust the viscosity of the PBI/PPA casting solution with identical monomer or polymer wt % charges. For the same polymer

content in the casting solution, the viscosity of the PBI/PPA casting solution decreased with increasing *meta*-PBI content in the copolymer. However, this was ultimately limited by the upper solubility limit of the composition. As shown in Table 1,

**Table 1. Polymer Solution Characteristics and Membrane Composition**

monomer charge wt % (molar ratio <i>meta</i> : <i>para</i> )	polymer wt % in casting solution	IV (dL/g)	polymer wt % in the membranes	PA wt % in the membranes	PA/PBI r.u.
7 (5:1)	5.6	2.45	14.9	54.3	12
7 (5:2)	5.6	2.78	14.0	54.4	12
7 (1:1)	5.6	1.60	10.8	66.8	19.5
10 (7:1)	8.0	3.67	17.5	52.6	9.5
10 (4:1)	8.0	3.77	17.3	51.7	9.4
<i>para</i> -PBI	1.6	3–5	5.0	56.6	30
<i>meta</i> -PBI	6.8	1.8	10	65	20.4

at 50% *para* content, the maximum monomer concentration achieved was 7 wt %, and this composition had to be cast prematurely (i.e., at low IV) to avoid precipitation or solidification of the polymerization solution.

The inherent viscosities of all *meta/para*-PBI polymers that did not exhibit early solidification during the polymerization were above 2.0 dL/g, similar to *para*-PBI polymers prepared via the PPA process and higher than *meta*-PBI polymers used for the conventionally imbibed PBI membranes (typically 0.6–0.8 dL/g). Generally, these inherent viscosities indicate that the synthesized copolymers achieved high molecular weights.<sup>28</sup>

**Membrane Characterization.** The proton conductivities of PA doped *meta/para*-PBI and *para*-PBI membranes made by the PPA process are shown in Figure 1. The *para*-PBI

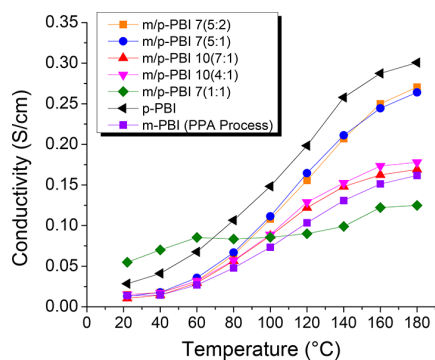


**Figure 1.** Proton conductivities of the *meta/para*-PBI copolymer membranes made from different monomer ratios and charges. Both *para*-PBI and *meta*-PBI are included for reference.

membranes prepared by the PPA process had high phosphoric acid doping levels (~30 PA/PBI r.u.), engendering the high measured proton conductivities of ~0.30 S/cm at 180 °C. However, even with relatively low PA doping levels, 12 and 10 PA/PBI r.u., the *meta/para*-PBI copolymers still had relatively high conductivities ranging from 0.26 to 0.17 S/cm at 180 °C, respectively. The measured high proton conductivities for these membranes is consistent with previously reported comparisons between conventionally imbibed and PPA processed membranes.<sup>22</sup>

Typically, the mechanical properties for *para*-PBI membranes with acid loadings of 25–30 PA/PBI r.u. (<5 wt % *para*-PBI) are 2 MPa tensile strength and 0.5 MPa Young's modulus. The phosphoric acid doping levels of the *meta/para*-PBI membranes were ~10 PA/PBI r.u., considerably lower than the *para*-PBI membranes, resulting in stronger membranes (7 MPa tensile strength and 11 MPa Young's modulus) and were similar to the membranes prepared by the conventionally imbibed process.<sup>13,22,29</sup> Figure 2 shows the

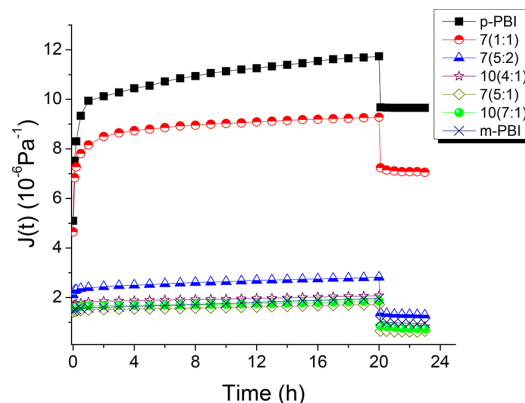


**Figure 2.** Creep deformation of *meta/para*-PBI copolymers compared to *para*- and *meta*-PBI homopolymers. Membranes were conditioned for 24 h at 180 °C. Strain was recorded under a static compression load for 20 h at 180 °C.

high-temperature creep properties of the high solids content *meta/para*-PBI, *meta*-PBI, and *para*-PBI membranes. When considering the critical membrane creep properties, both the steady-state recoverable compliance,  $J_s^0$  (creep compliance extrapolated to  $t = 0$ ), and creep rate,  $dJ/dt$ , indicate that the high solids membranes are more mechanically durable materials under compressive loads. The improved mechanical properties are likely due to the combined effects of the higher polymer content in the membrane, high molecular weights of the copolymer, and the copolymer composition.

**Fuel Cell Performance.** *Meta/para*-PBI synthesized at 10 wt % monomer charge with a 7:1 ratio of *meta/para* isomers was selected for further studies due to its high mechanical properties and proton conductivity. The membrane was constructed into a membrane electrode assembly (MEA) by first dipping into an 85% phosphoric acid bath for <30 s and then hot pressing between two Pt/C electrodes with 1 mg/cm<sup>2</sup> Pt loading on the anode and 1 mg/cm<sup>2</sup> Pt alloy loading on the cathode (BASF Fuel Cell, Inc.). The short-term acid dipping of the membrane into acid was conducted to wet the membrane surface and reduce interfacial resistances between the membrane and electrodes. The MEA was assembled into a single cell fuel cell and tested at 180 °C with hydrogen and air or oxygen at 1.2 and 2.0 stoichiometric flows, respectively. The gases were supplied at atmospheric pressure and dry (without external humidification). Figure 3 shows the polarization curves for the high solids membrane with both H<sub>2</sub>/air and H<sub>2</sub>/oxygen, which are slightly lower than *para*-PBI and consistent with the slightly lower conductivity. At 0.2 A/cm<sup>2</sup> using H<sub>2</sub>/air (1.2/2.0 stoichiometries), the potential was 0.676 V, and using H<sub>2</sub>/O<sub>2</sub> (1.2/2.0 stoichiometries) the potential was 0.758 V. At ~0.6 A/cm<sup>2</sup> the high solids membrane MEA exhibited mass transfer losses. However, very little optimization of MEA

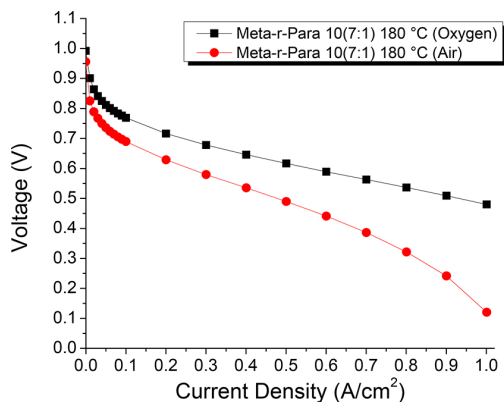


**Figure 3.** *Meta/para*-PBI 10(7:1) copolymer fuel cell performance data: (red circles) 180 °C  $\text{H}_2/\text{air} = 1.2/2.0$  stoichiometric flows, (black squares) 180 °C  $\text{H}_2/\text{O}_2 = 1.2/2.0$  stoichiometric flows; no external humidification.

pressing conditions has been conducted for these new membranes compared to the extensive development for *para*-PBI-based MEAs.

Long-term steady-state durability tests were performed on a membrane with the same selected copolymer ratio and monomer charge (10 wt % monomer charge at 7:1 *meta:para*). The test was performed at 160 °C, 0.2  $\text{A}/\text{cm}^2$ , using  $\text{H}_2/\text{air}$  at 1.2:2.0 stoichiometric ratios. Figure 4 shows the voltage

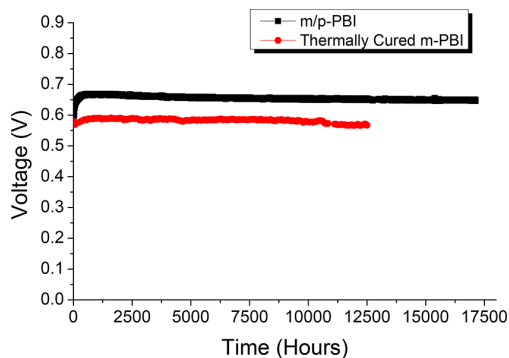


**Figure 4.** Long-term steady-state (0.2  $\text{A}/\text{cm}^2$ ) durability test of *meta/para*-PBI (7:1) copolymer (top curve) using  $\text{H}_2/\text{air} = 1.2/2.0$  stoichiometric flows at 160 °C compared to Sondergaard et al. for a thermally cured *meta*-PBI (bottom curve,  $\text{H}_2/\text{air} = 2.0/4.0$  stoichiometric flows at 160 °C).<sup>29</sup>

response under constant current conditions. The copolymer membrane showed excellent long-term stability at constant current density, running over 17,500 h before a catastrophic (flooding) event in the building resulted in an irrecoverable fuel cell test. The voltage decay for this MEA measured from  $\sim 5500$  h to end-of-life was  $0.69 \mu\text{V h}^{-1}$ , a value much lower than previously reported for *para*-PBI ( $\sim 6 \mu\text{V h}^{-1}$ ).<sup>30,31</sup> Recently, Sondergaard et al. reported long-term durability of a thermally cross-linked *meta*-PBI membrane prepared by the conventional imbibing process. They recorded a voltage degradation rate of  $0.5 \mu\text{V h}^{-1}$  for the first 9200 h of operation, and  $5.0 \mu\text{V h}^{-1}$  for the next 3800 h of operation. Both studies indicate that PBI membranes have great potential

for meeting the requirements of many devices for long-term durability.

Figure 5 shows the phosphoric acid evaporative loss for the first 4500 h of the test. The PA evaporative loss rate at the

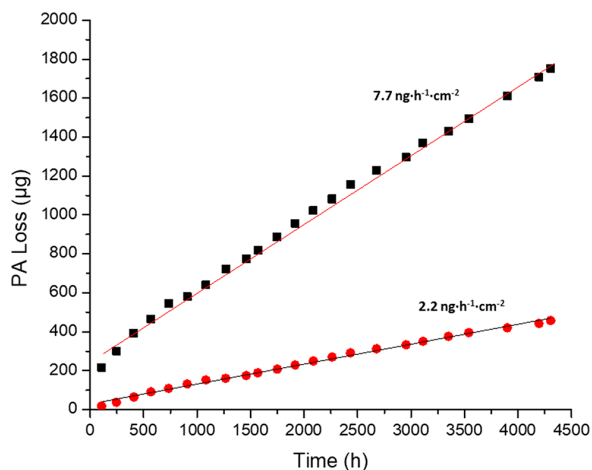


**Figure 5.** PA loss rates from the anode (red circles) and cathode (black squares) of the *meta/para*-PBI copolymer measured during steady-state fuel cell operation at 0.2  $\text{A}/\text{cm}^2$  and 160 °C.

anode and cathode were 2.2 and  $7.7 \text{ ng cm}^{-2} \text{ h}^{-1}$ , respectively. The amount of PA lost from the cathode was expectedly higher than that from the anode due to water vapor generation at the cathode during operation. At these PA loss rates, the total amount of acid lost from the membrane for a 40000 h lifetime would represent  $<1.5\%$  of the total acid in the original membrane. The movement of phosphoric acid in conventionally imbibed PBI membranes has been studied and showed that the migration rate of phosphoric acid was highly dependent on current density and the amount of free acid in the membrane.<sup>32</sup> However, experimental studies of phosphoric acid loss on PBI gel membranes under various conditions, for example, steady-state, start–stop, and current cycling, along with the work presented here all suggest that PA loss is not the most likely cause of performance degradation and failure under these time constraints.<sup>9,10,22,26</sup>

**Electrochemical Hydrogen Pump Operation.** The voltage required to pump pure  $\text{H}_2$  across the membrane showed a distinct linear dependence on current density, which was directly related to the resistance across the cell. *para*-PBI displayed lower voltages than the *meta/para*-PBI copolymer consistent with its higher proton conductivity. Interestingly, the expected trend of the voltage decreasing with increasing temperature is observed for the *meta/para* copolymer membrane but reversed for the *para*-PBI membrane. This unexpected trend is apparently due to the “softness” of the *para*-PBI membrane at the higher temperatures (see discussion on compression creep properties). SEM studies were conducted to examine the cross section of the membranes after completion of the hydrogen pump studies at 200 °C. For comparison, both membranes were measured to be  $\sim 200 \mu\text{m}$  after MEA compression and fabrication. However, after identical test protocols at 200 °C, the membrane thickness was  $104 \mu\text{m}$  for the *meta/para* copolymer membrane versus  $39 \mu\text{m}$  for the *para*-PBI membranes. Thus, the increase in voltage for the *para*-PBI membranes is consistent with the loss of

phosphoric acid and the resulting decrease in conductivity experienced under the compressive forces during full cell operation. Electrochemical measurements with these cells showed that the membrane resistance increased for the *para*-PBI membrane as the temperature increased from 160 to 200 °C (10.45 to 12.21 mohm), while the interface resistance remained constant at 1.5 mohm.

The MEAs were also subjected to hydrogen purification tests using a reformat test gas (30% H<sub>2</sub>, 3% CO, and 67% N<sub>2</sub>, mol %) supplied at 1.25 stoichiometric hydrogen flow on the anode and without a sweep gas on the cathode at 200, 180, and 160 °C (Figure 7). These tests clearly demonstrate two critical factors that affect electrochemical hydrogen purification, membrane conductivity, and Pt catalyst tolerance to CO. At all temperatures, the higher conductivity of *para*-PBI membranes compared to the *meta/para*-PBI membrane results in much lower voltages and thus lower power requirements for hydrogen purification. These effects were also obvious from the data in Figure 6 using pure hydrogen. However, the

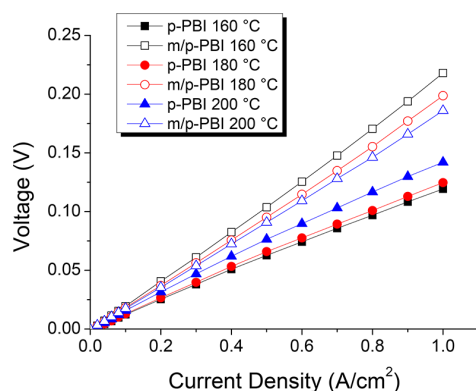


**Figure 6.** Electrochemical pump polarization curves for *meta/para*-PBI copolymer (7:1) and *para*-PBI membranes using humidified hydrogen (anode gas humidified at 1.6% RH).

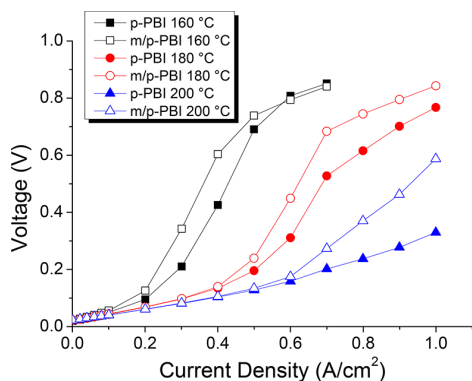


**Figure 7.** Electrochemical pump polarization curves for *meta/para*-PBI (7:1) copolymer and *para*-PBI membranes using a humidified reformat (30% H<sub>2</sub>, 3% CO, and 67% N<sub>2</sub>) test gas (anode gas humidified at 1.6% RH), 1.25 stoichiometry to H<sub>2</sub>. Anode and cathode held at 7.5 psi back-pressure.

temperature effects on Pt tolerance to CO, especially using a dilute hydrogen source, are prominent. The reversibility of CO binding to Pt dominates the performance of the device, and both membranes show much improved operation (lower

voltages and power requirements) at 180 °C compared to 160 and 200 °C compared to both 180 and 160 °C. Previous work on CO poisoning of Pt in phosphoric acid environments indicates that substantial differences in polarization losses and surface coverage of CO on Pt are observed in this temperature range and at this CO level, consistent with our hydrogen purification data.<sup>33</sup> Under these high-temperature operating conditions and increased pressure, we expect membrane creep to be accelerated limiting the lifetime of the MEA. When the combined effects of high proton conductivity and high operational temperatures are considered (*para*-PBI at 180 °C), hydrogen purification can be efficiently performed using a dilute hydrogen feedstream with large amounts of CO, producing a fairly pure hydrogen product. For example, at a target current density of 0.5 A/cm<sup>2</sup>, hydrogen purification from this mixed gas required ~100 mV. The purity of the separated hydrogen was measured via an Agilent 490 micro gas chromatograph in-line with the cathode exhaust. With handmade MEAs, hydrogen purity was typically found to be >99% with ~5 ppm carbon monoxide crossover and ppm levels of nitrogen gas from the mixture as well.

## CONCLUSION

PBI copolymers based on commercially available monomers were synthesized and characterized as membranes for fuel cells and related electrochemical devices. As the solubility of the copolymers in PPA increased, higher monomer charges could be used which resulted in higher polymer solids content in the cast membranes. However, the balance of meta- and para-oriented monomers also had an effect on membrane conductivity and short-term creep properties that are used to predict long-term durability. A copolymer composition was chosen for further studies that balanced the properties of ionic conductivity, polymer solids content in the membrane, and low creep compliance. Fuel cell performance was shown to be comparable to *para*-PBI. However, the long-term steady-state test resulted in an exceptionally low degradation rate measured over a 2 year run time and was ascribed to the low mechanical creep of the high solids content membrane. However, such correlations are hard to precisely make due to the lack of membrane creep and long-term performance data available in the literature. This work hopes to demonstrate the need for further exploration of membrane mechanical properties and their impact on long-term viability in electrochemical devices. The copolymers also performed effectively in an electrochemical hydrogen separation device, demonstrating the low power requirements for separating and purifying hydrogen without the need for large pressure differentials required for diffusion-based membranes and tolerance to catalyst poisons such as CO when operated at temperatures of 160 °C or higher.

## AUTHOR INFORMATION

### Corresponding Author

\*E-mail [benice@sc.edu](mailto:benice@sc.edu).

### ORCID

Andrew T. Pingitore: 0000-0002-0860-2909

Brian C. Benicewicz: 0000-0003-4130-1232

### Funding

The authors gratefully acknowledge BASF New Business for financial support of this work.

## Notes

The authors declare no competing financial interest.

## ACKNOWLEDGMENTS

The authors appreciate useful discussions with J. Belack and F. Doetz (BASF) during the course of this work.

## REFERENCES

- (1) Mader, J.; Xiao, L.; Schmidt, T.; Benicewicz, B. C. Polybenzimidazole/Acid Complexes as High-Temperature Membranes. *Adv. Polym. Sci.* **2008**, *216* (FuelCells II), 63–124.
- (2) Xiao, L.; Zhang, H.; Scanlon, E.; Ramanathan, L. S.; Choe, E. W.; Rogers, D.; Apple, T.; Benicewicz, B. C. High-Temperature Polybenzimidazole Fuel Cell Membranes via a Sol-Gel Process. *Chem. Mater.* **2005**, *17*, 5328–5333.
- (3) Gulledge, A. L.; Gu, B.; Benicewicz, B. C. A New Sequence Isomer of AB-Polybenzimidazole for High-Temperature PEM Fuel Cells. *J. Polym. Sci., Part A: Polym. Chem.* **2012**, *50*, 306–313.
- (4) Asensio, J. A.; Gomez-Romero, P. Recent Developments on Proton Conducting Poly(2,5-benzimidazole) (AB-PBI) Membranes for High Temperature Polymer Electrolyte Membrane Fuel Cells. *Fuel Cells* **2005**, *5*, 336–343.
- (5) Li, X.; Qian, G.; Chen, X.; Benicewicz, B. C. Synthesis and Characterization of a New Fluorine-Containing Polybenzimidazole (PBI) for Proton-Conducting Membranes in Fuel Cells. *Fuel Cells* **2013**, *13*, 832–842.
- (6) Qian, G.; Benicewicz, B. C. Synthesis and Characterization of High Molecular Weight Hexafluoroisopropylidene-Containing Polybenzimidazole for High-Temperature Polymer Electrolyte Membrane Fuel Cells. *J. Polym. Sci., Part A: Polym. Chem.* **2009**, *47*, 4064–4073.
- (7) Yu, S.; Benicewicz, B. C. Synthesis and Properties of Functionalized Polybenzimidazoles for High-Temperature PEMFCs. *Macromolecules* **2009**, *42*, 8640–8648.
- (8) Mader, J. A.; Benicewicz, B. C. Sulfonated Polybenzimidazoles for High Temperature PEM Fuel Cells. *Macromolecules* **2010**, *43*, 6706–6715.
- (9) Molle, M. A.; Chen, X.; Ploehn, H. J.; Benicewicz, B. C. High Polymer Content 2,5-Pyridine-Polybenzimidazole Copolymer Membranes with Improved Compressive Properties. *Fuel Cells* **2015**, *15*, 150–159.
- (10) Molle, M. A.; Chen, X.; Ploehn, H. J.; Fishel, K. J.; Benicewicz, B. C. High Polymer Content 3,5-Pyridine-Polybenzimidazole Copolymer Membranes with Improved Compressive Properties. *Fuel Cells* **2014**, *14*, 16–25.
- (11) Xiao, L.; Zhang, H.; Jana, T.; Scanlon, E.; Chen, R.; Choe, E. W.; Ramanathan, L. S.; Yu, S.; Benicewicz, B. C. Synthesis and Characterization of Pyridine-Based Polybenzimidazoles for High Temperature Polymer Electrolyte Membrane Fuel Cell Applications. *Fuel Cells* **2005**, *5*, 287–295.
- (12) Melchior, J. P.; Majer, G.; Kreuer, K. D. Why Do Proton Conducting Polybenzimidazole Phosphoric Acid Membranes Perform Well in High-Temperature PEM Fuel Cells? *Phys. Chem. Chem. Phys.* **2017**, *19*, 601–612.
- (13) Li, Q.; Hjuler, H. A.; Bjerrum, N. J. Phosphoric Acid Doped Polybenzimidazole Membranes: Physicochemical Characterization and Fuel Cell Applications. *J. Appl. Electrochem.* **2001**, *31*, 773–779.
- (14) Liao, J. H.; Li, Q. F.; Rudbeck, H. C.; Jensen, J. O.; Chromik, A.; Bjerrum, N. J.; Kerres, J.; King, W. Oxidative Degradation of Polybenzimidazole Membranes as Electrolytes for High Temperature Proton Exchange Membrane Fuel Cells. *Fuel Cells* **2011**, *11*, 745–755.
- (15) Dippel, T.; Kreuer, K. D.; Lassègues, J. C.; Rodriguez, D. Proton Conductivity in Fused Phosphoric Acid; A <sup>1</sup>H/<sup>31</sup>P PFG-NMR and QNS study. *Solid State Ionics* **1993**, *61*, 41–46.
- (16) Hickner, M. A.; Ghassemi, H.; Kim, Y. S.; Einsla, B. R.; McGrath, J. E. Alternative Polymer Systems for Proton Exchange Membranes (PEMs). *Chem. Rev.* **2004**, *104*, 4587–4611.
- (17) Savinell, R.; Yeager, E.; Tryk, D.; Landau, U.; Wainright, J.; Weng, D.; Lux, K.; Litt, M.; Rogers, C. A Polymer Electrolyte for Operation at Temperatures up to 200°C. *J. Electrochem. Soc.* **1994**, *141*, L46–L48.
- (18) Gokhale, R.; Asset, T.; Qian, G.; Serov, A.; Artyushkova, K.; Benicewicz, B. C.; Atanassov, P. Implementing PGM-free Electrocatalysts in High-Temperature Polymer Electrolyte Membrane Fuel Cells. *Electrochem. Commun.* **2018**, *93*, 91–94.
- (19) Garrick, T. R.; Wilkins, C. H.; Pingitore, A. T.; Mehlhoff, J.; Gulledge, A.; Benicewicz, B. C.; Weidner, J. W. Characterizing Voltage Losses in an SO<sub>2</sub> Depolarized Electrolyzer Using Sulfonated Polybenzimidazole Membranes. *J. Electrochem. Soc.* **2017**, *164*, F1591–F1595.
- (20) Perry, K. A.; Eisman, G. A.; Benicewicz, B. C. Electrochemical Hydrogen Pumping Using a High-Temperature Polybenzimidazole (PBI) Membrane. *J. Power Sources* **2008**, *177*, 478–484.
- (21) Peach, R.; Krieg, H.; Kruger, A.; Bessarabov, D.; Kerres, J. A. PBI-Blended Membrane Evaluated in High Temperature SO<sub>2</sub> Electrolyzer. *ECS Trans.* **2018**, *85*, 21–28.
- (22) Perry, K. A.; More, K. L.; Andrew Payzant, E.; Meisner, R. A.; Sumpster, B. G.; Benicewicz, B. C. A Comparative Study of Phosphoric Acid-Doped m-PBI Membranes. *J. Polym. Sci., Part B: Polym. Phys.* **2014**, *52*, 26–35.
- (23) Sondergaard, T.; Cleemann, L. N.; Becker, H.; Aili, D.; Steenberg, T.; Hjuler, H. A.; Seerup, L.; Li, Q. F.; Jensen, J. O. Long-Term Durability of HT-PEM Fuel Cells Based on Thermally Cross-Linked Polybenzimidazole. *J. Power Sources* **2017**, *342*, 570–578.
- (24) Chen, X. M.; Qian, G. Q.; Molle, M. A.; Benicewicz, B. C.; Ploehn, H. J. High Temperature Creep Behavior of Phosphoric Acid-Polybenzimidazole Gel Membranes. *J. Polym. Sci., Part B: Polym. Phys.* **2015**, *53*, 1527–1538.
- (25) Pilinski, N.; Rastedt, M.; Wagner, P. Investigation of Phosphoric Acid Distribution in PBI Based HT-PEM Fuel Cells. *ECS Trans.* **2015**, *69*, 323–335.
- (26) Schönberger, F.; Qian, G.; Benicewicz, B. C. Polybenzimidazole-Based Block Copolymers: From Monomers to Membrane Electrode Assemblies for High Temperature Polymer Electrolyte Membrane Fuel Cells. *J. Polym. Sci., Part A: Polym. Chem.* **2017**, *55*, 1831–1843.
- (27) Association, A. P. H. *Standard Methods for the Examination of Water and Wastewater*, 20th ed.; APHA: Washington, DC, 1999.
- (28) Hiorns, R. *Polymer Handbook*, 4th ed.; Brandup, J., Immergut, E. H., Eds.; John Wiley and Sons: New York, 1999; p 2250.
- (29) Søndergaard, T.; Cleemann, L. N.; Becker, H.; Aili, D.; Steenberg, T.; Hjuler, H. A.; Seerup, L.; Li, Q.; Jensen, J. O. Long-Term Durability of HT-PEM Fuel Cells Based on Thermally Cross-Linked Polybenzimidazole. *J. Power Sources* **2017**, *342*, 570–578.
- (30) Schmidt, T. J. Durability and Degradation in High-Temperature Polymer Electrolyte Fuel Cells. *ECS Trans.* **2005**, *1*, 19–31.
- (31) Schmidt, T. J.; Baurmeister, J. Durability and Reliability in High Temperature Reformed Hydrogen PEFCs. *ECS Trans.* **2006**, *3*, 861–869.
- (32) Eberhardt, S. H.; Marone, F.; Stampanoni, M.; Büchi, F. N.; Schmidt, T. J. Operando X-ray Tomographic Microscopy Imaging of HT-PEFC: A Comparative Study of Phosphoric Acid Electrolyte Migration. *J. Electrochem. Soc.* **2016**, *163*, F842–F847.
- (33) Dhar, H. P.; Christner, L. G.; Kush, A. K. Nature of CO Adsorption during H<sub>2</sub> Oxidation in Relation to Modeling for CO Poisoning of a Fuel Cell Anode. *J. Electrochem. Soc.* **1987**, *134*, 3021–3026.